Electronic Supplementary Information (ESI)

Controlled nucleation of ultrasmall MoO_3 nanoparticles on defective graphene for enhanced ammonia efficiency

Sakshi Bhardwaj,[a] Sumon Santra[a] and Ramendra Sundar Dey[a]*

[a]Institute of Nano Science and Technology, Sector-81, Knowledge city, S.A.S. Nagar (140306), Punjab, India.
*E-mail: rsdey@inst.ac.in

Table of Contents

1. Experimental Procedures

Chemicals and reagents

Melamine (Sigma Aldrich, $C_3H_6N_6$, AR), zinc powder (Sigma Aldrich, Zn, AR), sodium molybdate (Sigma Aldrich, $Na_2MoO_4 \cdot 2H_2O$) sodium sulfate (Sigma Aldrich, Na_2SO_4, AR), ammonium chloride (Sigma Aldrich, NH_4Cl, AR), hydrazine monohydrate (Sigma Aldrich, $N_2H_4 \cdot H_2O$, AR), sodium hydroxide (Sigma Aldrich, NaOH, AR), trisodium citrate (Sigma Aldrich, $Na_3C_6H_5O_7$, AR), sodium hypochlorite (Sigma Aldrich, NaClO, AR), phenol (Sigma Aldrich, C_6H_5OH, AR), and sodium nitroferricyanide (Sigma Aldrich, $Na_2[Fe(NO)(CN)_5]$, AR), Graphite strips (Excel Instruments), Every aqueous solution was made using DI water, and no additional purification was required for any of the compounds.

Synthesis procedure

Preparation of defective graphene (DG)

The preparation of DG was done using melamine as a precursor. An appropriate amount of melamine and zinc dust was taken in a 1:1 ratio. The mixture was ground thoroughly by the use of mortar and pestle to ensure a homogeneous powder mixture. Then the mixture was

placed in an alumina silicate boat and heated at a temperature of 800 °C under argon atmosphere for 2 h with ramp rate of 3 °C min^{-1} to form carbon framework. Thereafter, the as prepared carbon material was annealed at different temperatures 1050 °C under flowing argon gas and maintained at this temperature for 2 h to form defects by evaporation of Zn and nitrogen from the carbonized material (DG).

Preparation of Mo-DG

The preparation of Mo-DG was carried out in an ultrasonic setup. The DG produced from the above-mentioned pathway was taken in an appropriate amount in a vial. And was dispersed in an ethanol-water mixture with a 9:1 ratio. The mixture was sonicated for 4 hours to ensure uniform distribution of the DG in the solution. Then the solution was transferred to an ice bath maintaining the temperature to 0 ˚C in the ultrasonicator. After that, 150 µL of 1 mM of sodium molybdate, (optimized amount) was taken and added slowly to the DG dispersion over a period of 30 minutes and the sonication was carried in the ice bath condition for the next 6 hours. The resulting mixture was later centrifuged and washed to obtain the Mo-DG. The resulting material was stored for further characterization and use. The same sample was prepared under room temperature conditions (Mo-DG RT).

Instrumentation

A Bruker D8 Advances equipment was utilized to acquire a powder X-ray diffraction (PXRD) pattern, utilizing Cu-Kα (λ = 1.5406 Å) radiation in the 2θ range of 5° to 50°, while applying an acceleration voltage of 40 KV. An analytical method commonly known as X-ray powder diffraction (XRD) was used to study the structural and phase analysis of Mo-DG. The inductively coupled plasma–mass spectrometry (ICP-MS) was performed for the detection of the metal loading capacity in the material using Agilent 7850 ICP-MS. The surface morphology and elemental content of the as-synthesized nanomaterial were investigated using a Bruker X Flash 6130 paired with an Energy Dispersive X-ray Spectroscopy (EDS)-equipped JeolJSMIT300 scanning electron microscope. The elemental composition of the produced nanomaterial was determined by EDS measurements for additional examination. Utilizing the JEOL JEM-2100 apparatus, a high-resolution transmission electron microscope (HRTEM) was employed for nanoscale microscopic study.

The materials' Raman spectra were obtained using a WITEC Focus Innovations Alpha-300 Raman confocal microscope and a 532 nm excitation laser. Using FTIR equipment from

Agilent Technologies' Cary 600 series, Fourier transform infrared spectroscopy (FT-IR) was conducted at room temperature. The surface elemental composition and bonding arrangement of the generated samples were analyzed using X-ray photoelectron spectroscopy (XPS) spectrometer (K-Alpha 1063) instruments and Al-Kα radiation (1486.6 eV) in an ultrahigh vacuum chamber (7 X 10^{-9} torr). UV−vis−near infrared (NIR) (Cary 5000 UV−vis−NIR, model: G9825A CARY) spectrophotometer was used for UV−vis characterizations. ^{1}H spectra were measured using a 400 MHz Bruker Avance II 400 NMR spectrometer. Chemical shifts are represented in parts per million (δ) for samples in [D^{6}] DMSO, and are calibrated using tetramethylsilane as an internal reference.

2. The electrochemical study

The CHI 760E electrochemical workstation, which included chronoamperometry, cyclic voltammetry (CV), linear sweep voltammetry (LSV), and other techniques was used to measure every aspect of the electrochemical performance. In an H-Cell, the NRR experiment was conducted. Three electrode systems make up the H-Cell. The reference electrode (Ag/AgCl), counter electrode (coiled Pt wire), and the working electrode (a graphite plate with an area of 1*1 cm^2). In the cathodic chamber, the working and reference electrodes are linked, while the counter electrode is connected in the anodic chamber. All the potentials used are in RHE and can be related as:

$$E_{RHE} = E_{Ag/AgCl} + 0.0591\,pH + 0.210 \qquad eq.1$$

The Nafion-117 membrane intersection made up the H-Cell. The membrane is cleaned by treating it with an aqueous solution of 5% H_2O_2 for an extra hour at 80 °C after it has been boiled for an hour in ultrapure water. After that, it was immersed in 0.5 M H_2SO_4 for three hours at 80 °C, and then it was left in water for six hours.

Preparation of working electrode. For the preparation of catalyst ink, 5mg of the catalyst was dispersed in a 1:1 (v/v) mixture of IPA (0.5mL) and DI (0.5mL). The prepared catalyst was sonicated for a period of 2 hours in an ultrasonicator to avoid clumping up of the catalyst and blocking of active sites. Meanwhile, commercially obtained graphite sheets were cut into 1 * 1 cm^2. The copper wire connecting the graphite electrodes has been cleaned at both terminal ends to remove the oxide coatings. Following the ultrasonication process, 25 μ L of catalyst ink was dropped over the graphite surface and allowed to dry under an infrared lamp. The next day, the electrode was used for the electrocatalytic investigation.

3. N_2 purification and NH_3 detection

Purification of N_2 gas

The $^{14}N_2$ gas, which was purchased from Sigma Aldrich, was first passed through alkaline (0.1 M KOH) and subsequently acid (0.05 M H_2SO_4) traps to get rid of any possible impurities. This was done in anticipation that inadvertent NH_3 would be captured by the acid trap and NO_x impurities would be captured by the base trap. Using UV-vis spectroscopic methods, the pollutants in the gas, including NH_3 and NO_x, were comprehensively examined. Before the filtered gas was purged into the electrocatalytic cell, the input gas was collected and used to test for any other gaseous contamination using gas chromatography.

Ammonia detection by Indophenol blue method

In order to identify ammonia, an aliquot of 5 milliliters was extracted from the H-Cell's cathodic chamber. 20 µL of phenol (1 mg mL^{-1}) and 12.5 µL of sodium nitroferricyanide ($C_5FeN_6Na_2O$) were added to the aliquot, respectively. Subsequently, the solution's pH was brought to about 9.25 by adding 100 µL of NaOCl and using NaOH and trisodium citrate solution. The pH was then once more brought to 10 with the use of trisodium citrate solution and NaOH. After that, the solution combination was left to incubate for two hours in the dark. After incubation, the blue hue that these solution combinations produced was captured for UV Vis examination.

This was done in order to measure the ammonia produced by the electrocatalytic process. The amount of ammonia that was created was determined using the calibration curve from a set of solutions with known concentrations of NH_4Cl in 0.5 M Na_2SO_4. These solutions were supplemented with the previously specified reagents, and after an hour of incubation, the absorbance was determined.

Calculation of the Faradaic efficiency and yield of ammonia

The FE for NRR is the ratio of the total charge that flows through the electrodes during the electrolysis process to the electric charge needed to create NH_3. The amount of NH3 created is determined using the colorimetric method. The following is the formula for FE:

$$FE = \frac{3F \times C_{NH_3} \times V}{17 \times Q} \qquad eq.2$$

The number three in the equation above denotes the number of electrons required to create a single NH_3 molecule. where V is the volume of electrolyte used, Q is the total charge traveled through the electrodes, F is the Faraday's constant, and CNH^3 is the concentration of NH_3 generated.

The following formula provides the ammonia yield:

$$R_{NH_3} = \frac{C_{NH_3} \times V}{m \times t} \qquad eq.3$$

Here m represents the mass of the catalyst and t is the time of reaction.

$^{15}N_2$-isotope labelling experiment

Quantification of ammonia by the NMR study

analysis. This was subsequently added with 50 μL of 0.01 M maleic acid solution followed by DMSO-d6 and subjected to ^{1}H-NMR study. The obtained peaks were integrated and by using the following eq. 4, the concentration of NH_3 was quantified and matched with that obtained from UV–visible spectroscopic method.

$$\frac{I_{sample}}{I_{standard}} = \frac{H_{sample} * C_{sample}}{H_{standard} * C_{standard}} \qquad eq.4$$

where *I* stands for the integral values, H stands for the number of protons (4 in case of sample NH_4^+ and 2 in case of the vinylic protons of maleic acid) and *C* stands for the concentrations of the sample and standard (0.01 M for maleic acid).

Determination of NO_x

NOx pollution was measured using the N-(-1-naphthyl)-ethylenediamine dihydrochloride spectrophotometric method. To make the chromogenic agent, 0.5 g of sulfanilic acid was dissolved in 90 ml of deionized water and 5 ml of acetic acid. After adding 5 mg of N-(1-naphthyl)-ethylenediamine dihydrochloride, the mixture was raised to a volume of 100 ml. To keep light out, the prepared solution was covered. One milliliter of the chromogenic ingredient was mixed with four milliliters of the experimental solutions. For fifteen minutes, the resultant solution was stored in the dark.

Determination of Hydrazine

By using the Watt and Chrisp approach, hydrazine was discovered. 0.2 g of para-(dimethylamino) benzaldehyde was diluted in 10 mL of ethanol and 1 mL of concentrated HCl to provide the coloring agent for N_2H_4 detection. To the 2 mL of aliquot, 2 mL of the generated coloring agent was applied prior to performing the UV-vis characterization. After that, the combination was left to incubate in the dark for fifteen minutes. According to the matching Fig., there was a significant linear relationship between absorbance and NH_3 concentration.

4. Supporting Figures

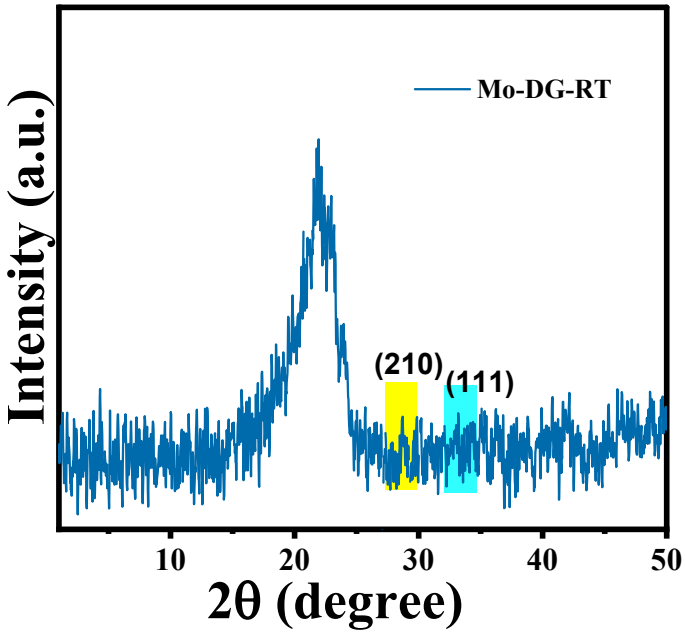

Fig. S1. XRD pattern of Mo-DG RT.

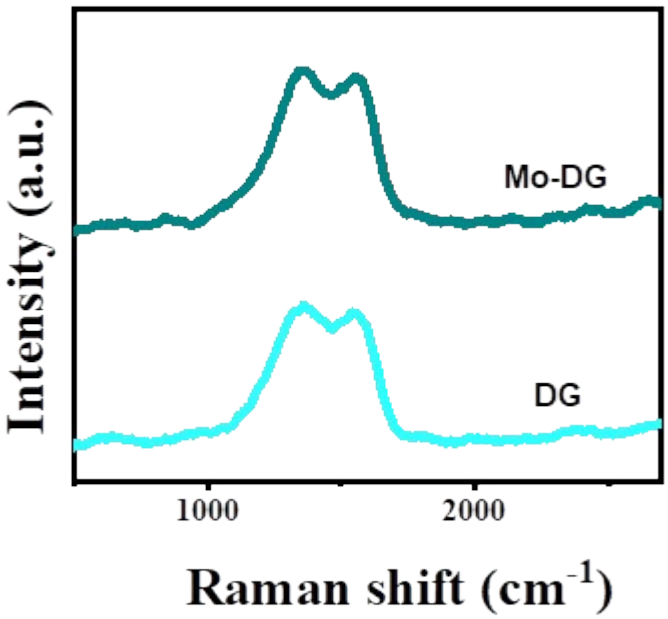

Fig. S2. Raman spectra of DG and Mo-DG.

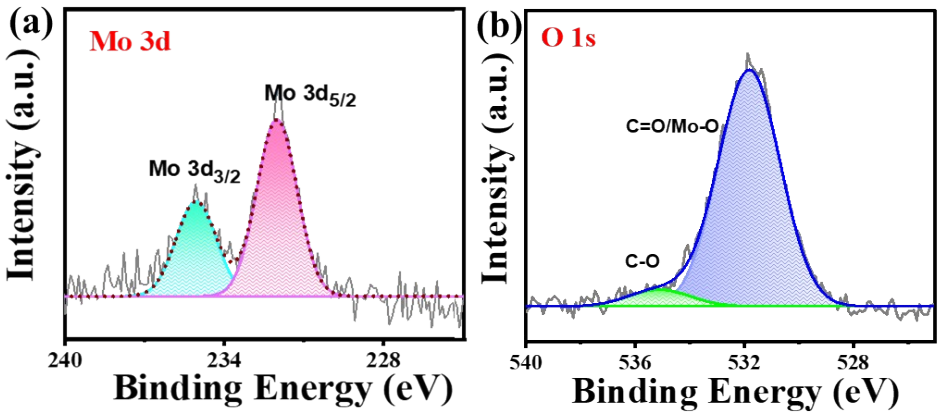

Fig. S3. (a) Deconvoluted Mo 3d spectra; (b) O 1s spectra of Mo-DG.

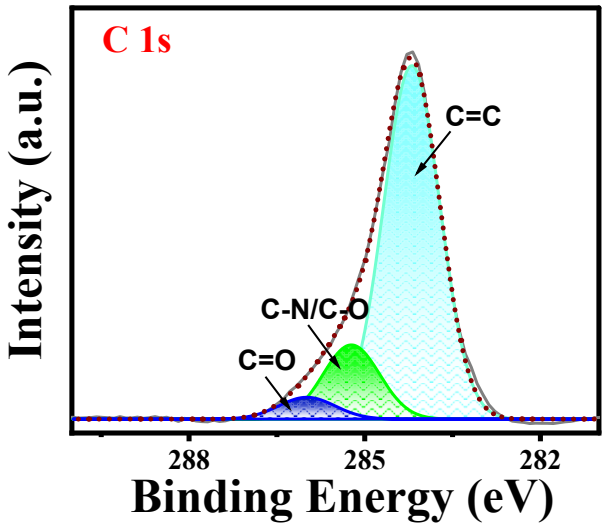

Fig. S4. Deconvoluted C 1s spectra of Mo-DG.

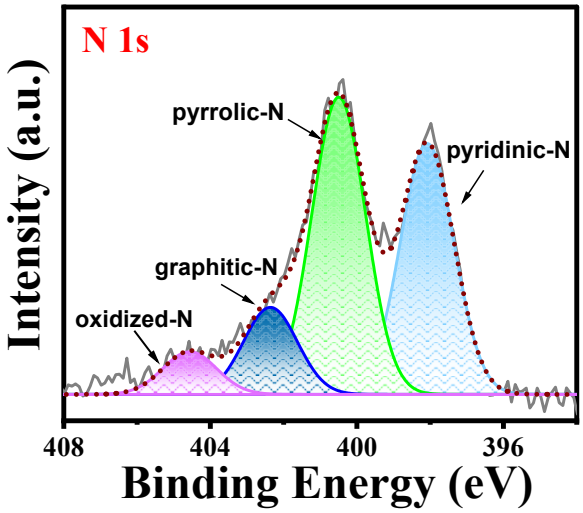

Fig. S5. Deconvoluted N 1s spectra of Mo-DG.

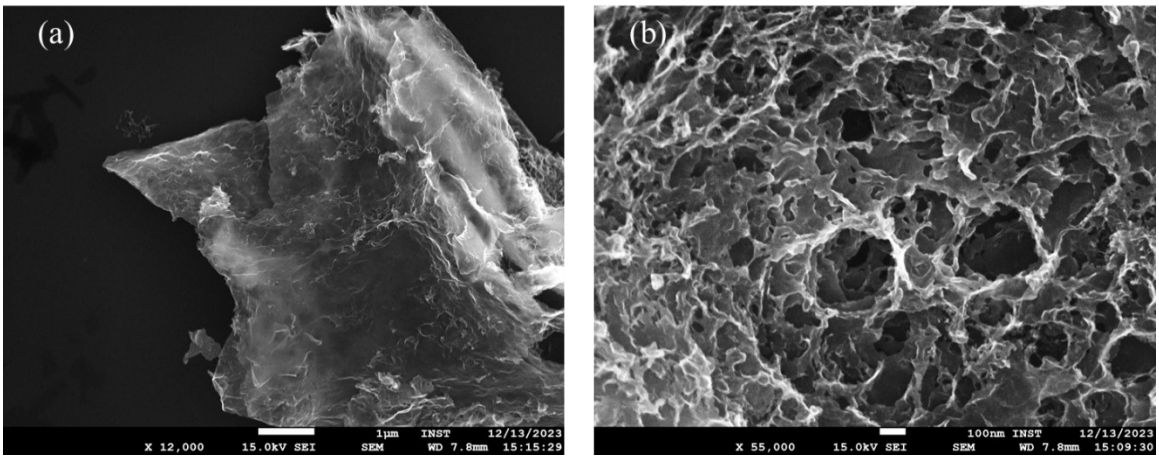

Fig. S6. (a, b) FESEM images of Mo-DG.

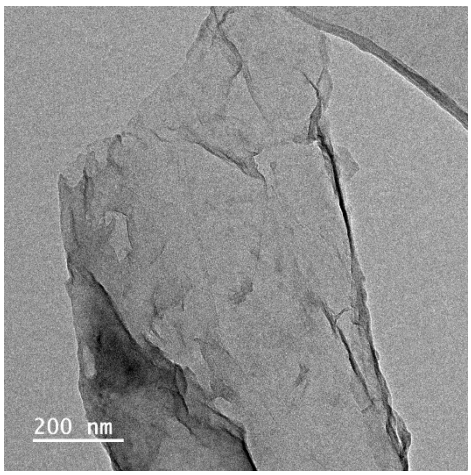

Figure S7. TEM image of Mo-DG.

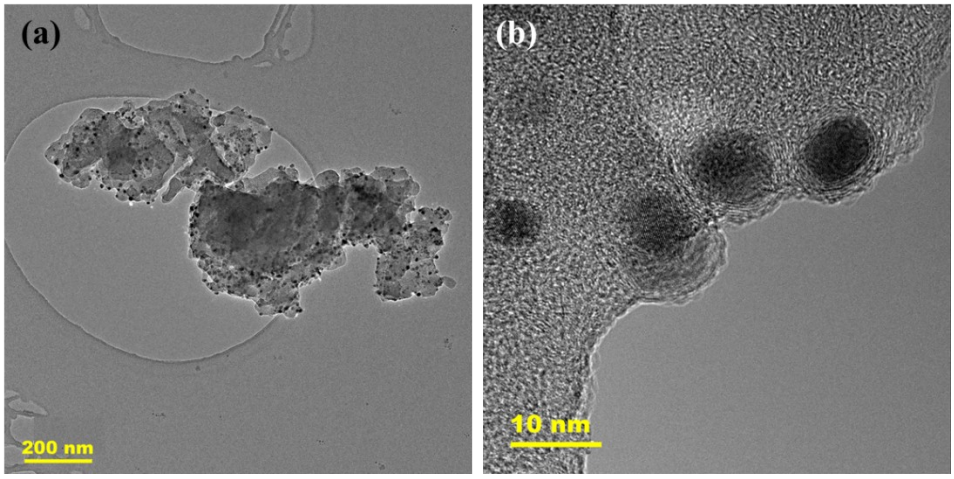

Fig. S8. (a) TEM image of Mo-DG RT; (b) HRTEM image of Mo-DG RT.

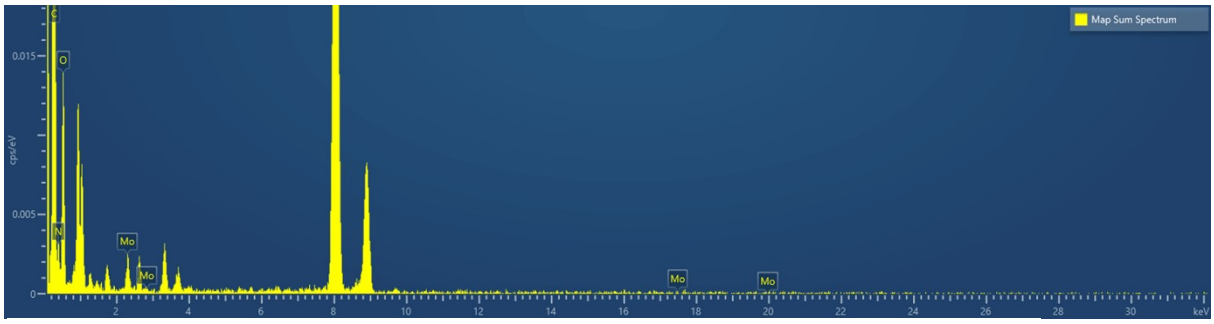

Figure S9. EDS image of Mo-DG.

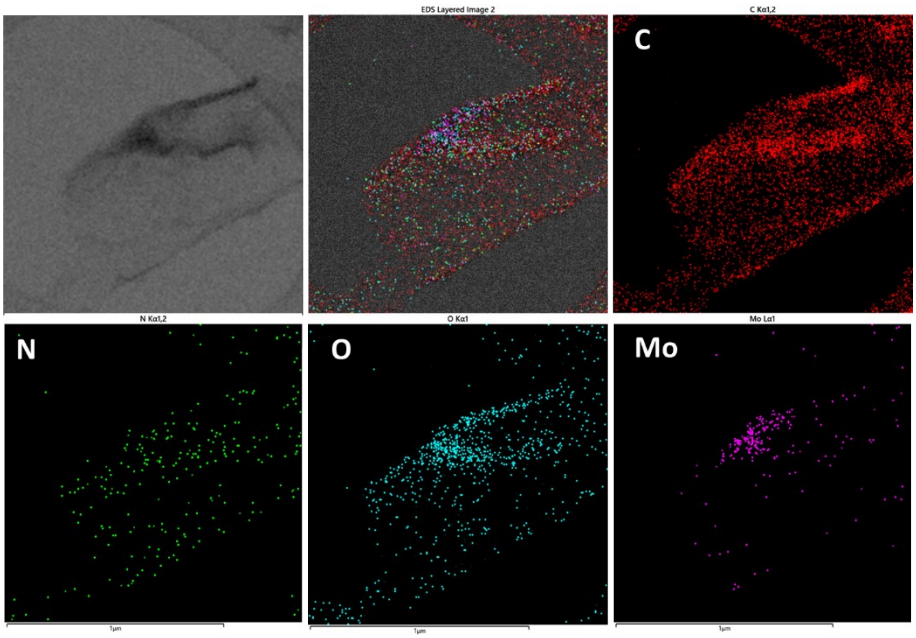

Figure S10. TEM mapping of Mo-DG.

Injection Details

Injection Name: NITROGEN_1 *Run Time (m* 6.00 *Vial Number:* 234 *Injection Volu*1.00
Injection Type: Unknown *Channel:* FID1+FID2+TCD *Instrument Method:* Analysis *Bandwidth:*
n.a.
Processing Method: Quantitative *Dilution Facto*1.0000
Injection Date/Time: 28-Oct-24 19:08 *Sample Weig*1.0000

Chromatogram

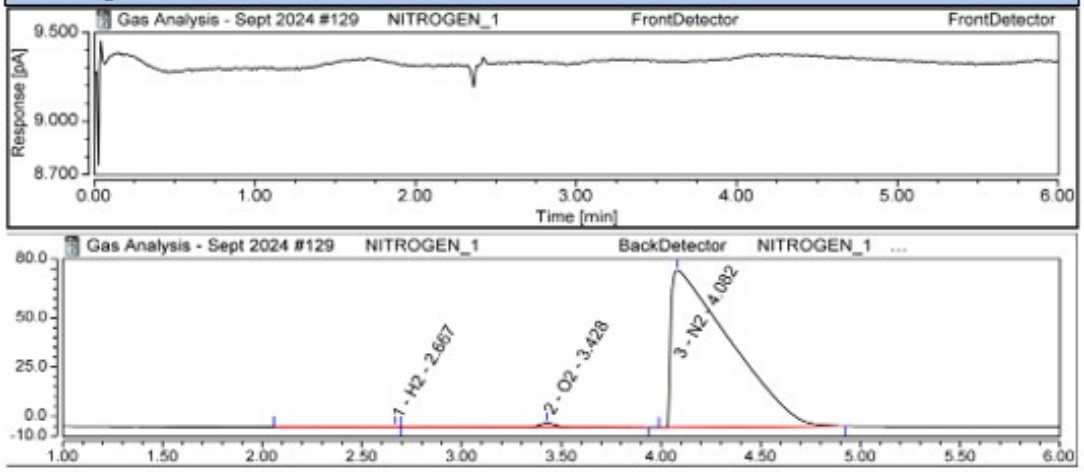

Integration Results

No.	Peak Name	Retention Time min	Area pA*min	Height pA	Relative Area%	Relative Height %	Amount n.a.
1	H2	2.667	0.016	0.007	0.06	0.01	48.4505
2	O2	3.428	0.337	2.147	1.22	2.62	9735.7978
3	N2	4.082	27.205	79.898	98.72	97.37	1006714.2731

Figure S11. Gas chromatographic report for the purity of nitrogen gas injected.

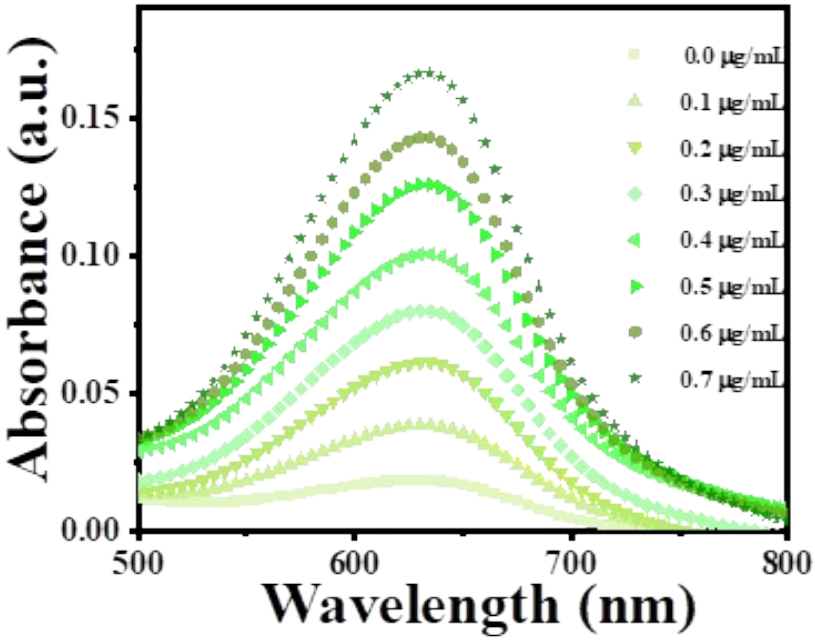

Figure S12. UV-vis absorption presenting the different known concentrations of NH_4^+ in 0.5 M Na_2SO_4 with indophenol blue indicator solutions after 2 h incubation under ambient conditions.

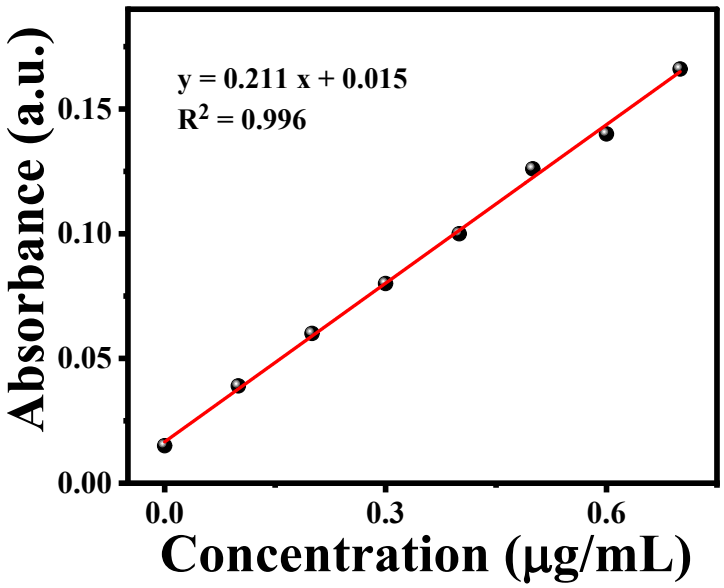

Figure S13. Calibration curve of ammonia–indophenol blue absorbance used in this study.

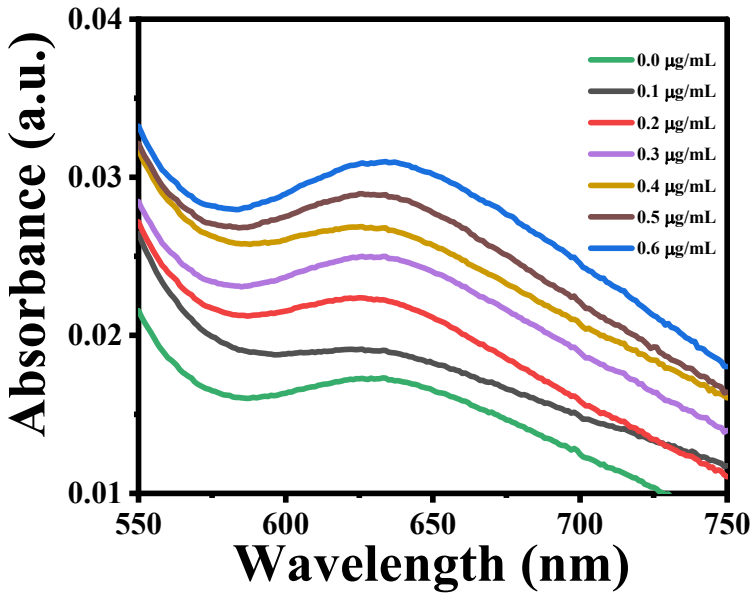

Figure S14. UV-vis absorption presenting the different known concentrations of NH_4^+ with indophenol-blue indicator in acid trap solutions after 2 h incubation under ambient conditions.

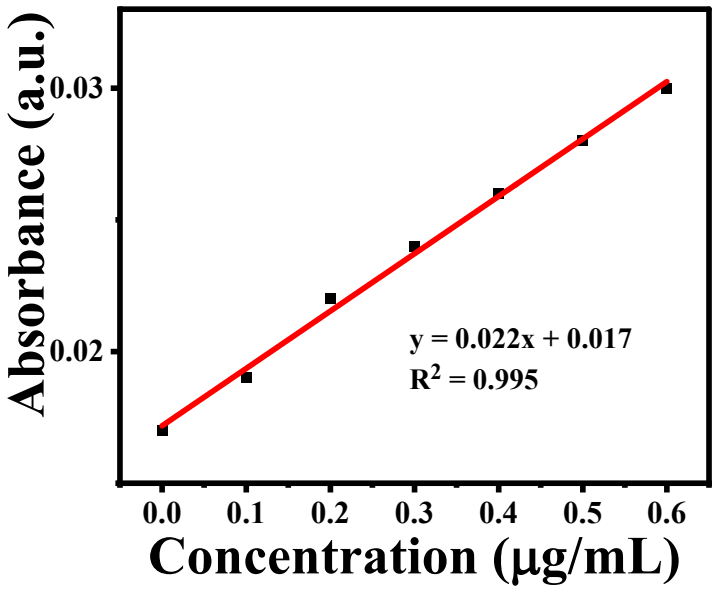

Figure S15. Calibration curve of ammonia – indophenol blue absorbance in acid trap solutions after 2 h incubation under ambient conditions.

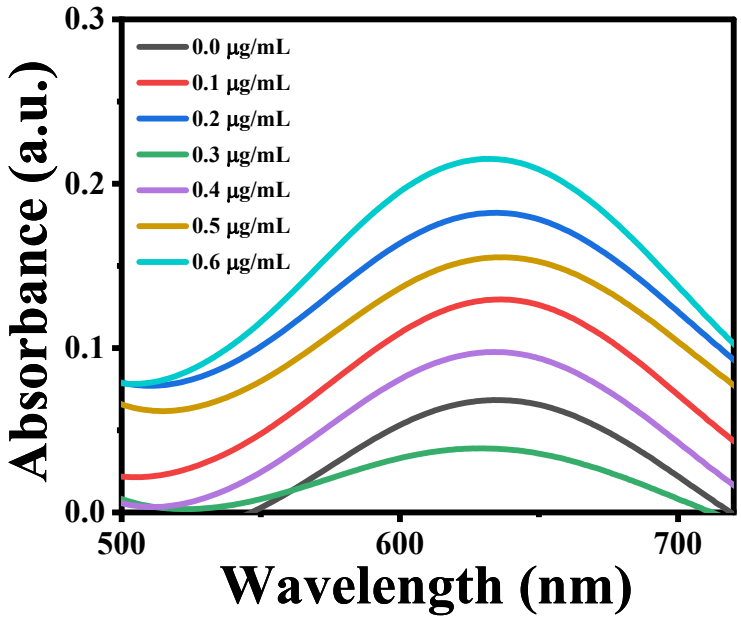

Figure S16. UV-vis absorption presenting the different known concentrations of NH_4^+ with indophenol-blue indicator in base trap solutions after 2 h incubation under ambient conditions.

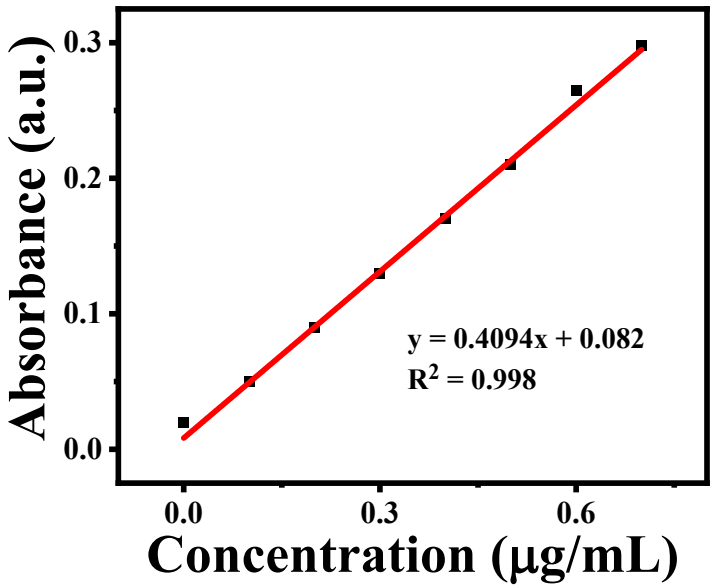

Figure S17. Calibration curve of ammonia – indophenol blue absorbance in base trap solutions after 2 h incubation under ambient conditions.

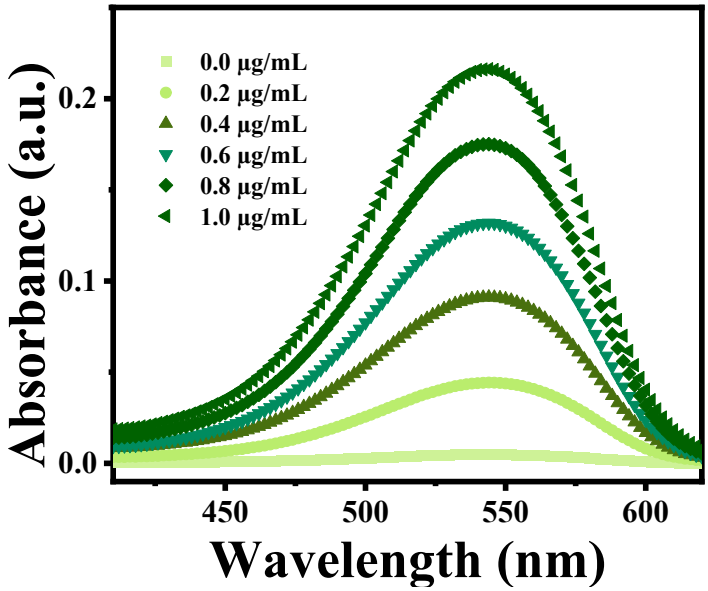

Figure S18. UV-vis absorption presenting the different known concentrations of NO_x with indophenol-blue indicator solutions after 2 h incubation under ambient conditions.

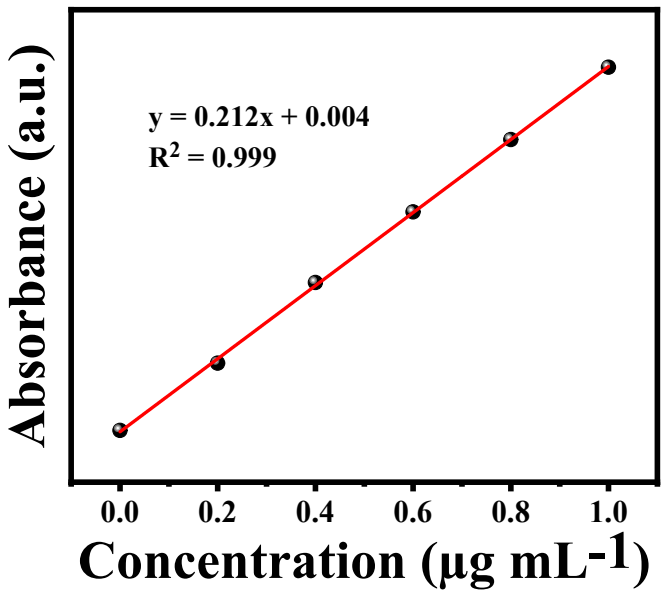

Figure S19. Calibration curve of ammonia – indophenol blue absorbance in NO_x solutions after 2 h incubation under ambient conditions.

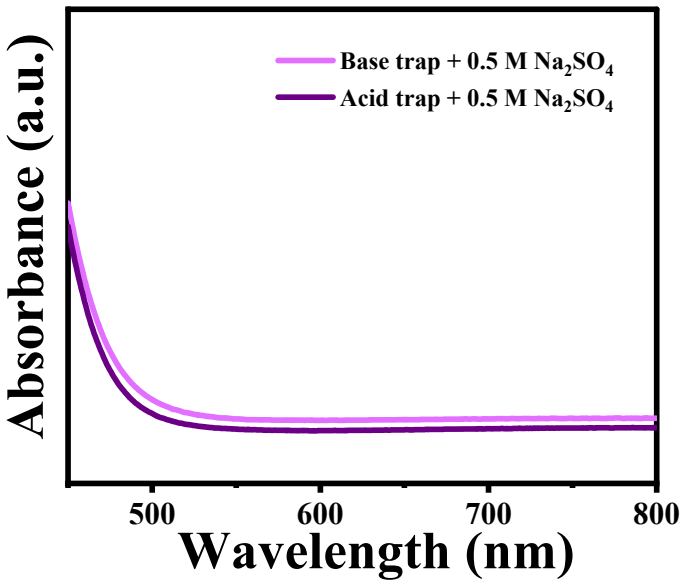

Figure S20. UV-vis absorption spectra of 0.1 M KOH (basic) and 0.05 M H_2SO_4 (acidic trap) + 0.5 M Na_2SO_4 under ambient conditions.

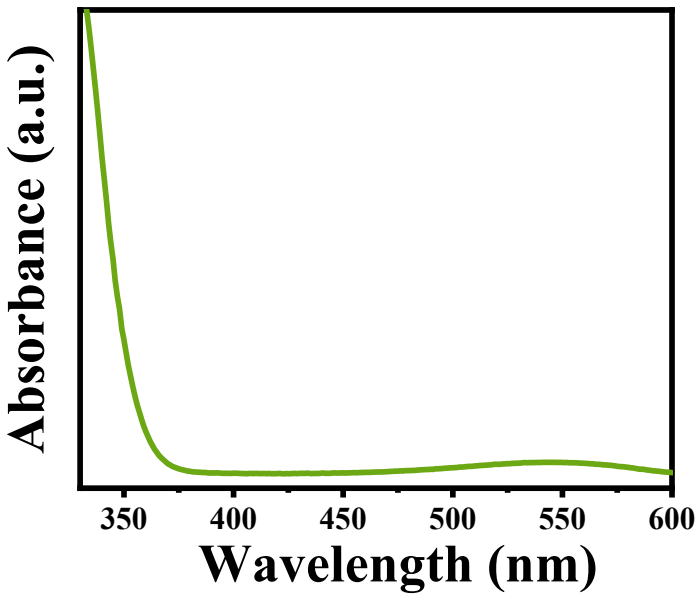

Figure S21. UV-vis absorption spectra of 0.1 KOH (basic trap) + 0.5 M Na_2SO_4 under ambient conditions for detection of NO_x.

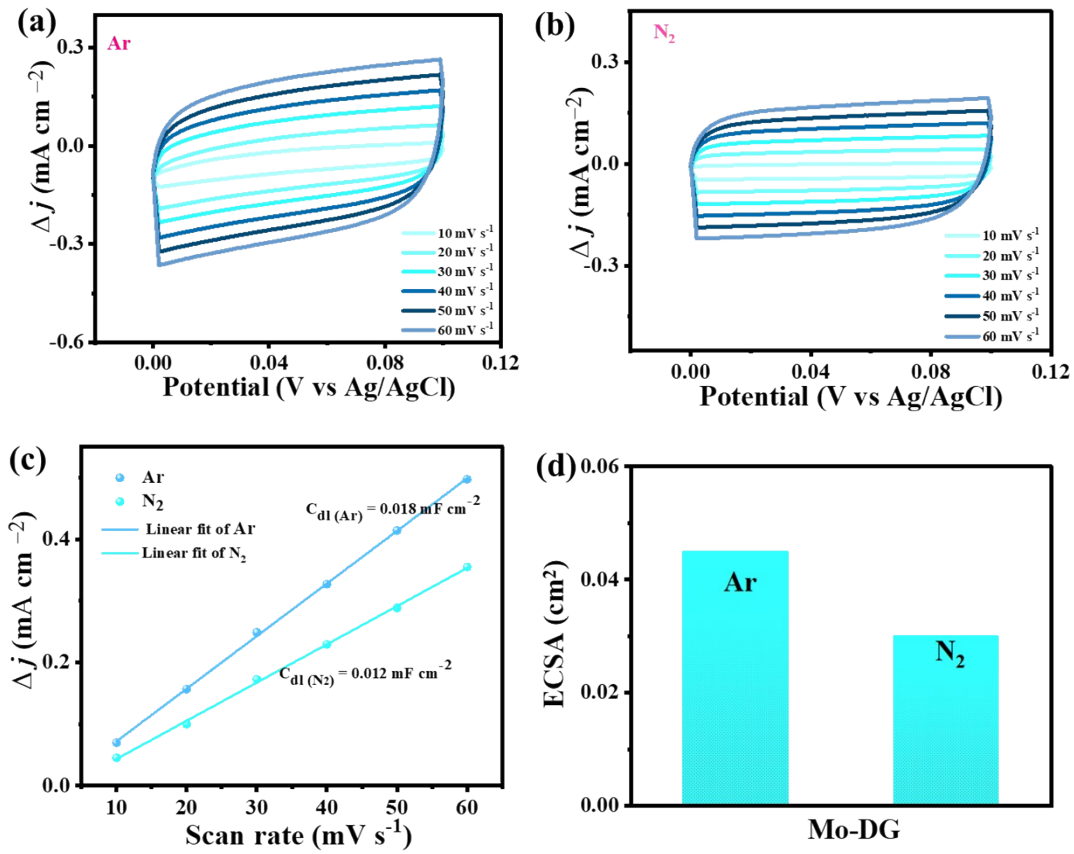

Figure S22. (a, b) CV curves at various scan rates (10 to 50 mV s^{-1}) in the non-Faradaic region for Mo-DG in Ar and N_2 saturated 0.5 M Na_2SO_4, respectively; (c) linear fits of Δj (difference of anodic and cathodic current densities) obtained from the CV curves**,** where the slope is twice the double-layer capacitance (C_{dl}); and (d) the bar plot showing the ECSA of Mo-DG in the presence of Ar and N_2.

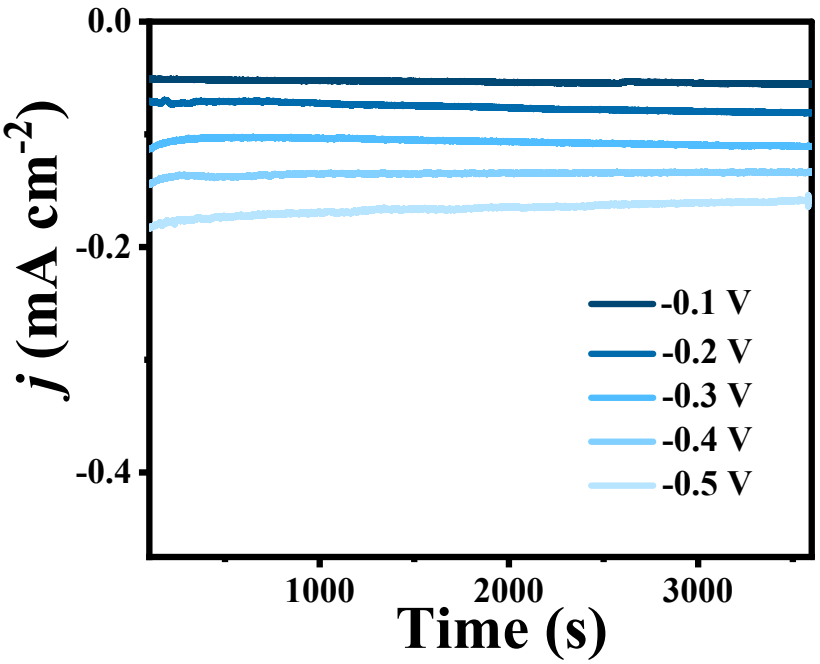

Figure S23. Chronoamperometric response of Mo-DG at different potentials in 0.5 M Na_2SO_4.

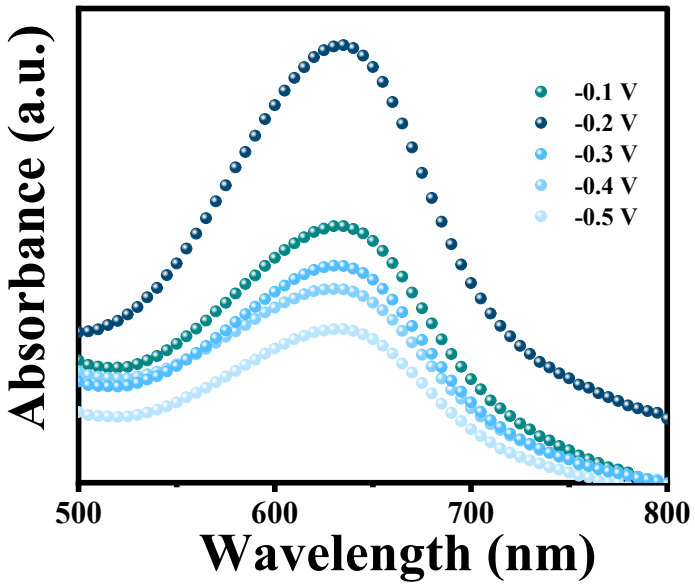

Figure S24. UV-vis absorption spectra of 0.5 M Na_2SO_4 containing different concentrations of NH_4^+ at different potentials with indophenol-blue indicator solutions after 2 h incubation under ambient conditions.

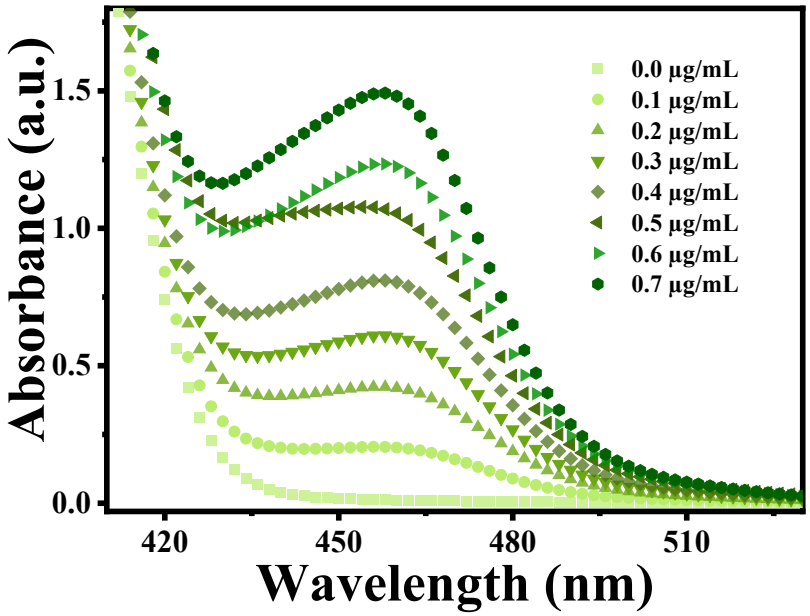

Figure S25. UV-vis absorption presenting the different known concentrations of N_2H_4 after 15 mins incubation under ambient conditions.

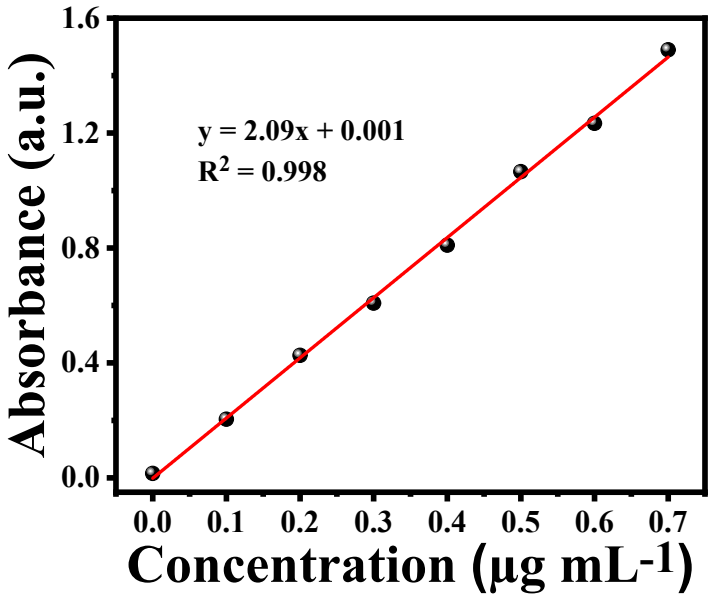

Figure S26. Calibration curve of hydrazine–absorbance used in this study.

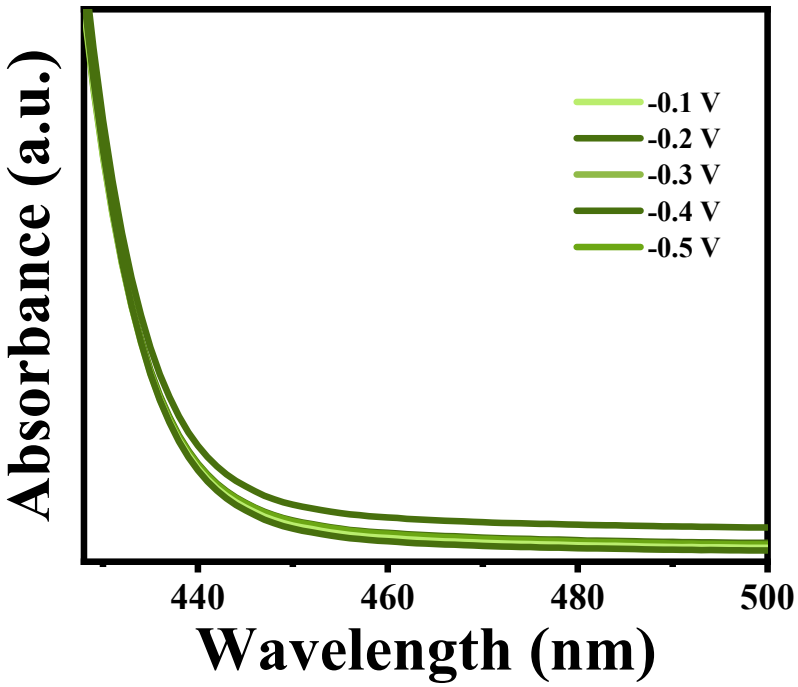

Figure S27. UV-vis absorption spectra of 0.5 M Na_2SO_4 containing different concentrations of N_2H_4 produced at different potentials after 15 mins of incubation under ambient conditions.

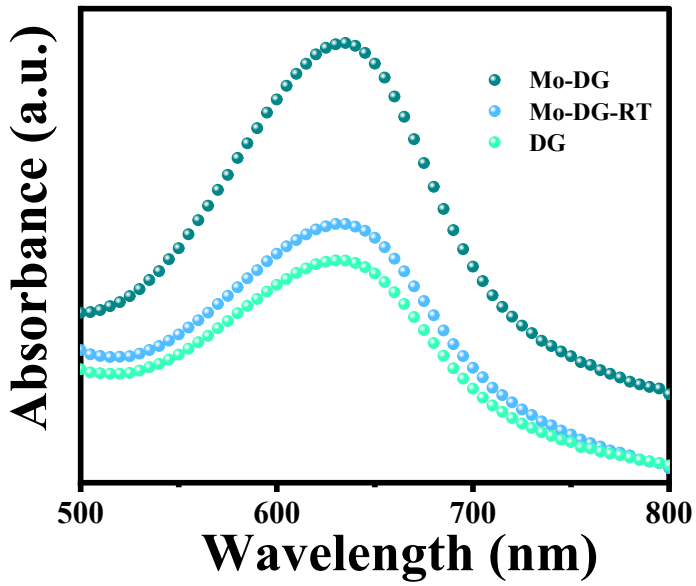

Figure S28. UV-vis absorption spectra of 0.5 M Na_2SO_4 containing different concentrations of NH_4^+ produced in the case of DG, Mo-DG-RT and Mo-DG electrocatalysts using indophenol-blue indicator solutions after 2 h incubation under ambient conditions.

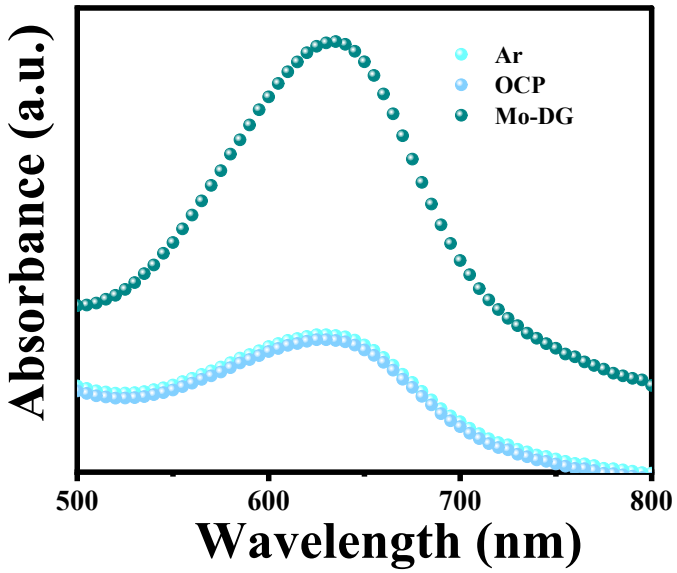

Figure S29. UV-vis absorption spectra of 0.5 M Na_2SO_4 containing different concentrations of NH_4^+ produced in argon and at OCP using indophenol-blue indicator solutions after 2 h incubation under ambient conditions.

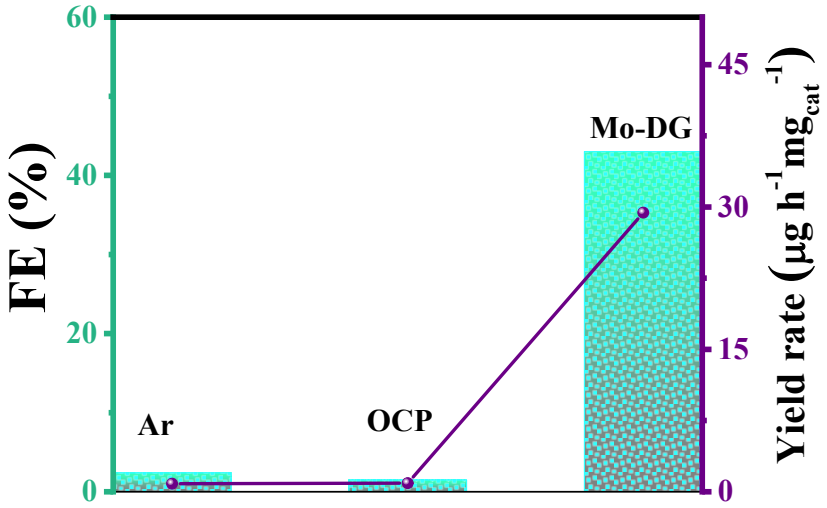

Figure S30. The bar plot presents the NRR performance of Mo-DG in Ar, N_2 media and at OCP.

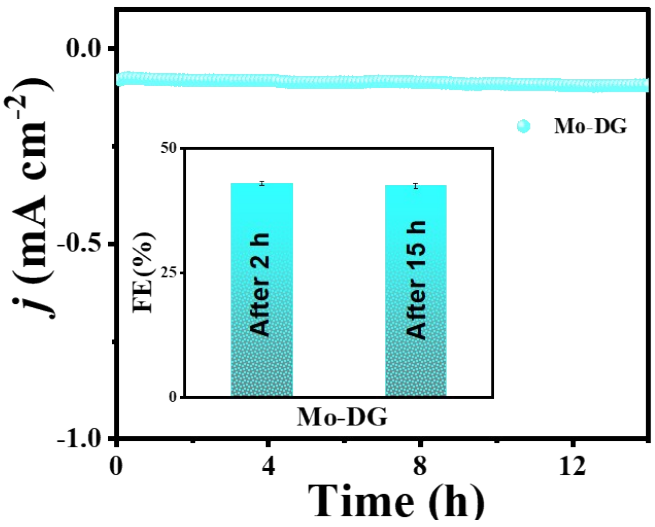

Figure S31. Stability of the Mo-DG catalyst for 15 h at -0.2 V, inset shows FE after 2 and 15 h.

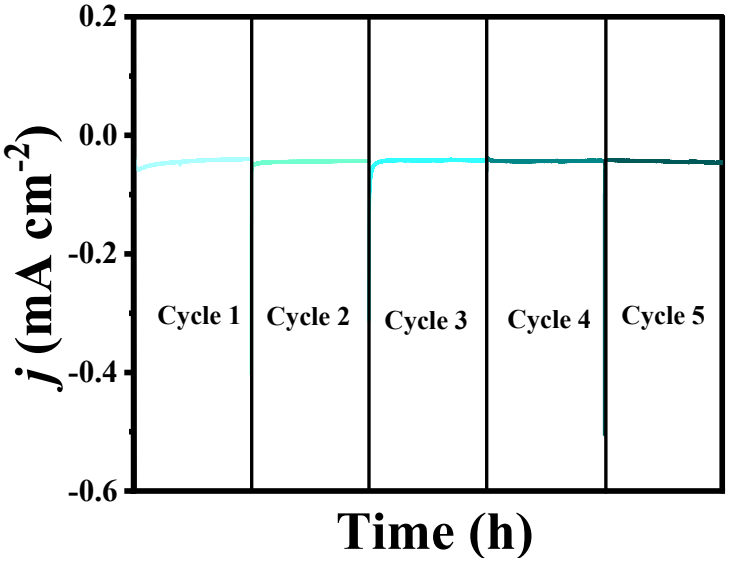

Figure S32. CA response of Mo-DG during five cycles of repeatability at -0.2 V potential in 0.5 M Na_2SO_4.

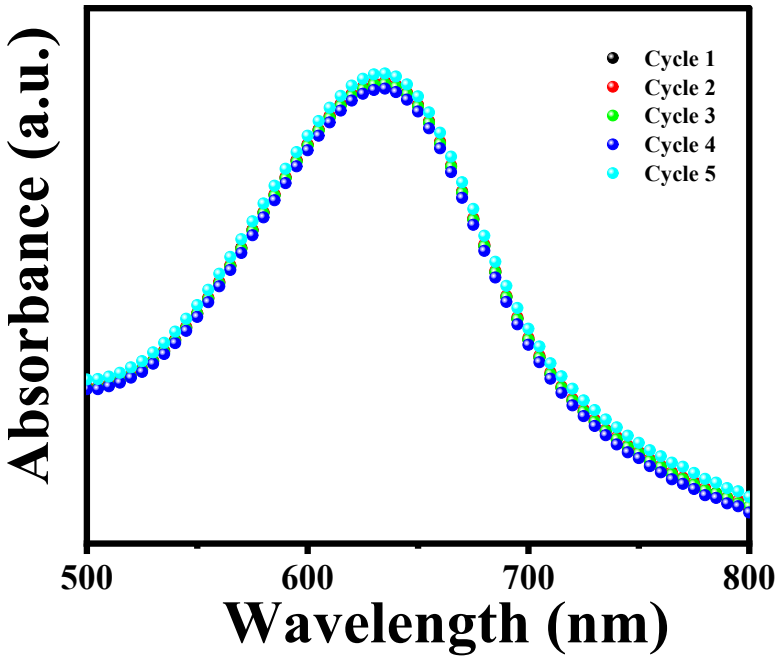

Figure S33. UV-vis absorption spectra of 0.5 M Na_2SO_4 containing NH_4^+ produced during different five cycles of repeatability at -0.2 V using indophenol-blue indicator solutions after 1 h incubation under ambient conditions.

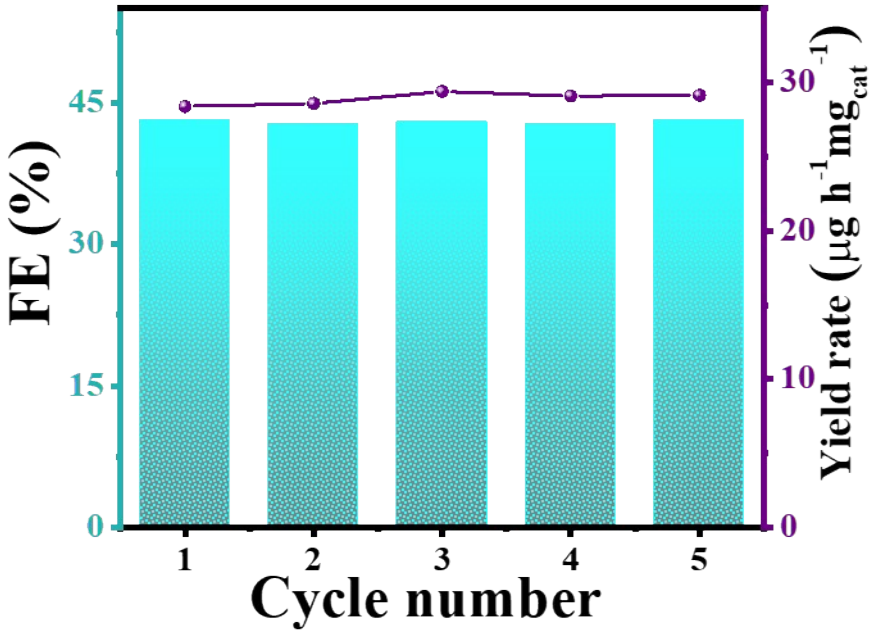

Figure S34. The bar plot presenting NRR performance of Mo-DG during five cycles.

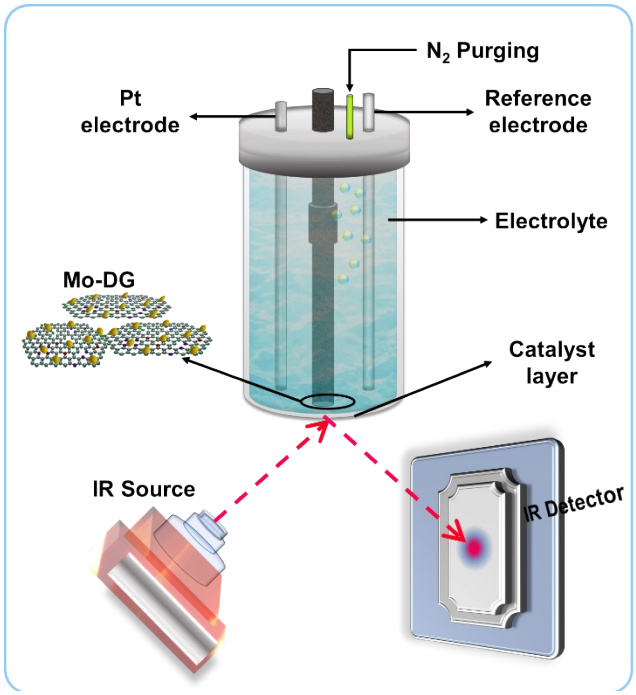

Figure S35. Schematic diagram of *in situ* ATR-IR cell used for electrochemical measurements during NRR.

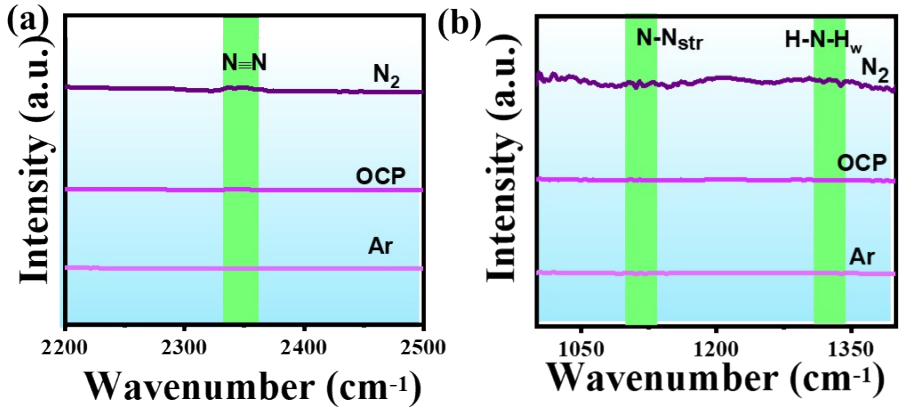

Figure S36. (a, b) The *in situ* ATR-FTIR spectra obtained for Mo-DG.

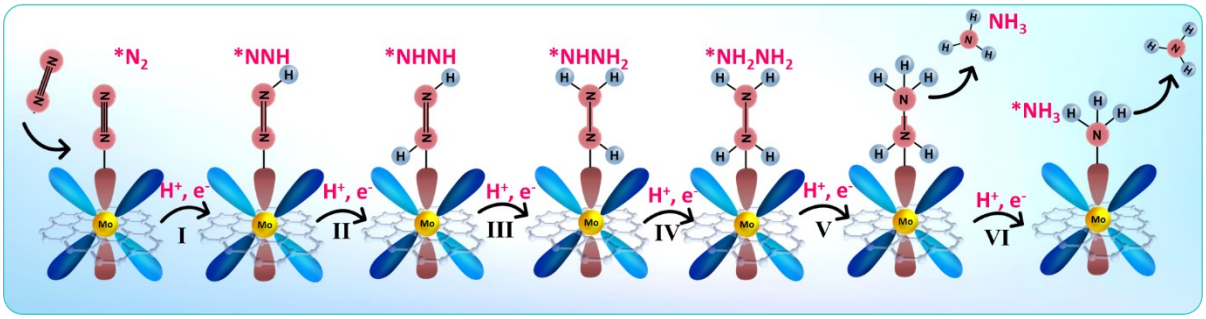

Figure S37. Associative mechanism followed on the surface of Mo-DG.

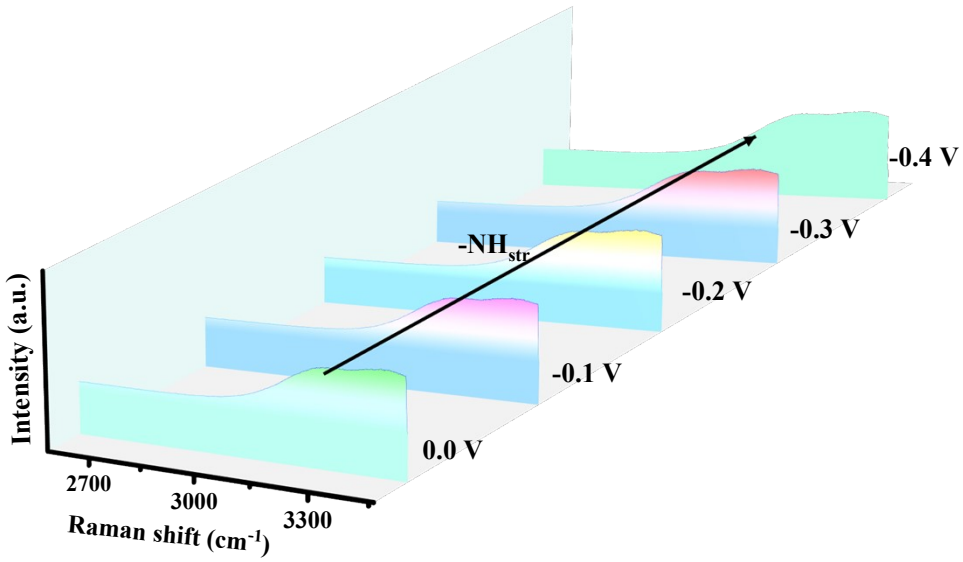

Figure S38. The *in situ* Raman spectra obtained for Mo-DG.

Table S1. Comparison table representing the NRR activity of Mo-DG and other literature reports.

Electrocatalyst	Electrolyte	Potential (RHE)	FE (%)	Yield rate	Ref.
Reduced graphene oxides with engineered defects	0.1 M HCl 0.1 M KOH	- 0.116 V - 0.166 V	22.0% 10.8%	7.3 µg·h-1 mg -1	[1]
Mo Single Atoms and Mo2C Nanoparticles on CNTs	0.005 M H_2SO_4	−0.25 V (*vs.* RHE)	7.1%	16.1 µg h^{-1} cm_{cat}^{-2}	[2]
Mo Single-Atom Sites on B/N Codoped Porous Carbon Nanotubes	0.1 M KOH	−0.4 V	13.27%	37.67 µg h^{-1} mg_{cat}^{-1}	[3]
Mo single atoms anchored on porous N-doped carbon	0.05 M H_2SO_4	−0.2 V	24.03%	15.34 µg h^{-1} mg^{-1}	[4]
Mo atoms anchored to nitrogen-doped porous carbon	0.1 M KOH	−0.3 V	14.6±1.6 %	34.0±3.6µg h^{-1} $mg_{cat.}^{-1}$	[5]
Mo-DG	**0.5 M Na_2SO_4**	**-0.2 V**	**43.1 %**	**28.4 µg h^{-1} $mg_{cat.}^{-1}$**	**This work**

References

1 M. Zhang, C. Choi, R. Huo, G. H. Gu, S. Hong, C. Yan, S. Xu, A. W. Robertson, J. Qiu, Y. Jung and Z. Sun, *Nano Energy*, 2020, **68**, 104323.

2 Y. Ma, T. Yang, H. Zou, W. Zang, Z. Kou, L. Mao, Y. Feng, L. Shen, S. J. Pennycook, L. Duan, X. Li, J. Wang, Y. Y. Ma, W. J. Zang, Z. K. Kou, S. J. Pennycook, J. Wang, L. Mao, X. Li, T. Yang, Y. P. Feng, H. Y. Zou, L. L. Duan and L. Shen, *Advanced Materials*, 2020, **32**, 2002177.

3 L. Shi, S. Bi, Y. Qi, R. He, K. Ren, L. Zheng, J. Wang, G. Ning and J. Ye, *ACS Catal*, 2022, **12**, 7655–7663.

4 K. Y. Hsiao, Y. H. Tseng, C. L. Chiang, Y. De Chen, Y. G. Lin and M. Y. Lu, *ACS Appl Nano Mater*, 2023, **6**, 10713–10724.

5 L. Han, X. Liu, J. Chen, R. Lin, H. Liu, F. Lü, S. Bak, Z. Liang, S. hunzheng Zhao, E. Stavitski, R. R. Adzic, H. L. Xin, J. P. Chen, H. X. Liu, F. Lü, J. Luo, D. LHan, D. QLin, D. Bak, Z. X. Liang, R. R. Adzic, D. ZZhao, D. Stavitski and H. L. Xin, *Angewandte Chemie International Edition*, 2019, **58**, 2321–2325.